UNIVERSITY OF WEST BOHEMIA

Applied and Computational Mechanics 1 (2007) 541 - 548

Applied and Computational Mechanics

Residual stress simulation of circumferential welded joints

R. Melicher [a], J. Meško [b], P. Novák [a], M. Žmindák [a,*]

[a] *Department of Applied Mechanics, Faculty of Mechanical Engineering, University of Žilina, Univerzitná 1, 010 26 Žilina, Slovak Republic*
[b] *Department of Technological Engineering, Faculty of Mechanical Engineering, University of Žilina, Univerzitná 1, 010 26 Žilina, Slovak Republic*

Received 10 September 2007; received in revised form 10 October 2007

Abstract

Residual stresses are an important consideration in the component integrity and life assessment of welded structure. The welding process is very complex time dependent physical phenomenon with material nonlinearity. The welding is a thermal process with convection between fluid flow and welding body, between welding body and environment. Next type of boundary conditions is radiation and thermo-mechanical contact on the outer surface of gas pipe in the near of weld. The temperature variation so obtained is utilised to find the distribution of the stress field.

In this paper, a brief review of weld simulation and residual stress modelling using the finite element method (FEM) by commercial software ANSYS is presented. Thermo-elastic-plastic formulations using a von Mises yield criterion with nonlinear kinematics hardening has been employed. Residual axial and hoop stresses obtained from the analysis have been shown. The commercial FEM code ANSYS was used for coupled thermal-mechanical analysis.

Keywords: residual stress, thermal process in welding, numerical model, finite element method

1. Introduction

The welding process is very complex time dependent physical phenomenon with material nonlinearity. The nonlinear effects are caused nonlinear dependency of thermal conductivity coefficient, specific heat coefficient, density of material on temperature. Another nonlinearities are caused with specialized boundary conditions. From the thermal cycle point of view, the arc welding performs the strong concentration of the heat source onto the small area of the welding materials [1]. The intense heat of the arc melts both parts to be welded at the point of the metal electrode, which supplies filler metal for the weld. The heat source moves in the desired direction by the certain velocity. After the melting, the weld rapidly cools. The change of temperature depends on distance from welding centre. The boundary conditions and the thickness of the base material essentially determine the cooling velocity. This velocity was significantly increased due to the strong convection of the heat into the flowing water inside the test plates.

The structural changes of the material depend on the material temperature properties. Therefore the welding parts contain finally a few structural phases, which of the physical and mechanical properties are different. The technological welding procedures depend mostly on desired properties of the weld in the service conditions [9].

Usually the weld does perform the region with a highest hardness, and heat affected zones (HAZ) represent the material with a pure properties. HAZ is crucial to the strength of the

*Corresponding author. Tel.: +421415132962, e-mail: Milan.Zmindak@fstroj.uniza.sk

welded joint since the cracking and fracture occur inside the HAZ region. The thermal stresses due to expansion and contraction are the other effect of the temperature history during the welding process [2, 3, 8]. The thermal stress analysis is out of the scope of this contribution. The changes of the microstructure and macrostructure together with a residual stress of the welded materials characterize the quality and reliability of the welded joint [5].

2. Theory background

2.1. Thermal analysis

In the thermal analysis, the transient temperature field T of the welded plate is a function of time t and the spatial coordinates (x, y, z), and is determined by the non-linear heat transfer equation for body in fig. 1.

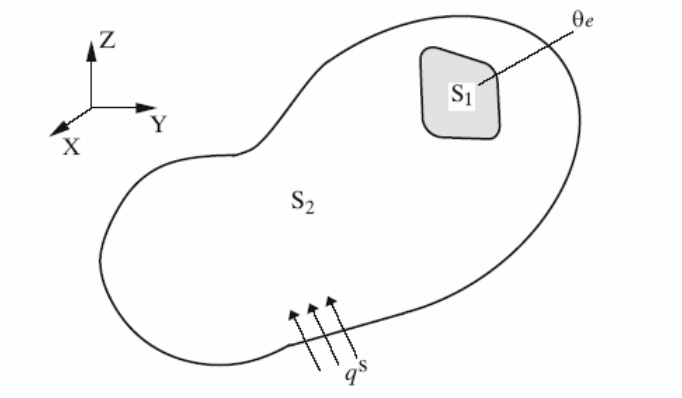

Fig. 1. Body subjected to heat transfer.

$$\frac{\partial}{\partial x}\left(k_x \frac{\partial T}{\partial x}\right)+\frac{\partial}{\partial x}\left(k_x \frac{\partial T}{\partial x}\right)+\frac{\partial}{\partial x}\left(k_x \frac{\partial T}{\partial x}\right)=-q^B, \tag{1}$$

where

T - temperature [K]
q^B - is rate of heat generated per unit volume [W/m^3]
k - heat conductivity [W/(mK)]

At surfaces of body the following conditions must be satisfied

$$T = T_e \qquad \text{on } S_1, \tag{2}$$

$$k_n = \frac{\partial T}{\partial n} = q^S \quad \text{on } S_2. \tag{3}$$

The equation (2) express that the temperature can be prescribed at specific points and surfaces of the body, denoted by S_1. The equation (3) is the heat flow input can be prescribed at specific points and surfaces. In equation (3) S_2 are convection boundary conditions where

$$q^S = h\left(T_e - T^S\right), \tag{4}$$

where h [W/m^{2}K] being convection coefficient (possibility temperature depend), T_e is the environmental (external) temperature, and T^S is the body surface temperature. For nonlinear heat transfer the k and h are temperature dependent.

For transient problems the heat stored within the material is given by

$$q^C = mc_p\dot{T}\,, \tag{5}$$

where c_p [J/kgK] is the material heat capacity and the superposed dot denotes differentiation respect to time. Then nonlinear equation has form

$$\frac{\partial}{\partial x}\left(k_x\frac{\partial T}{\partial x}\right)+\frac{\partial}{\partial x}\left(k_x\frac{\partial T}{\partial x}\right)+\frac{\partial}{\partial x}\left(k_x\frac{\partial T}{\partial x}\right)+q^B=\rho c_p\frac{\partial T}{\partial t}\,. \tag{6}$$

2.2. Thermal stresses

When incoming to material dilatation then relation between stress and strain for linear material is

$$\boldsymbol{\sigma}=\mathbf{E}\boldsymbol{\varepsilon}^{el}=\mathbf{E}\left(\boldsymbol{\varepsilon}-\boldsymbol{\varepsilon}^{th}\right), \tag{7}$$

where $\boldsymbol{\sigma}$ is stress vector

$$\boldsymbol{\sigma}=\left[\sigma_{xx}\ \ \sigma_{yy}\ \ \sigma_{zz}\ \ \tau_{xy}\ \ \tau_{yz}\ \ \tau_{zx}\right]^T, \tag{8}$$

$\boldsymbol{\varepsilon}$ is total deformation and $\boldsymbol{\varepsilon}^{th}$ is deformation vector from temperatures and $\mathbf{E}$ is elasticity matrix

$$\boldsymbol{\varepsilon}=\left[\varepsilon_{xx}\ \ \varepsilon_{yy}\ \ \varepsilon_{zz}\ \ \gamma_{xy}\ \ \gamma_{yz}\ \ \gamma_{zx}\right]^T. \tag{9}$$

Equation (7) in inverse form is

$$\boldsymbol{\varepsilon}=\boldsymbol{\varepsilon}^{\mathbf{th}}+\mathbf{E}^{-1}\boldsymbol{\sigma}\,. \tag{10}$$

For the 3D case, thermal strain tensor is

$$\boldsymbol{\varepsilon}^{\mathbf{th}}=\Delta T\left[\alpha_x\ \alpha_y\alpha_z\,0\,0\,0\right]^T, \tag{11}$$

where α_x, α_y, α_z, [K^{-1}] are thermal coefficients of expansion in *x*, *y*, *z* direction, $\Delta T = (T\text{-}T_{REF})$, *T* is current temperature.
Flexibility matrix $\mathbf{E}^{-1}$ is

$$\mathbf{E}^{-1}=\begin{bmatrix} 1/E_{xx} & -\nu_{xy}/E_{xx} & -\nu_{xz}/E_{xx} & 0 & 0 & 0\\ -\nu_{yx}/E_{xx} & 1/E_{yy} & -\nu_{yz}/E_{yy} & 0 & 0 & 0\\ -\nu_{zx}/E_{xx} & -\nu_{zy}/E_{zz} & 1/E_{zz} & 0 & 0 & 0\\ 0 & 0 & 0 & 1/G_{xy} & 0 & 0\\ 0 & 0 & 0 & 0 & 1/G_{yz} & 0\\ & & & & & 1/G_{xz} \end{bmatrix}, \tag{12}$$

where E_{xx}, E_{yy}, E_{zz} - are Young's modules in the *x*, *y*, resp. *z* direction, ν_{xy} - is major Poisson's ratio, ν_{yx} - is minor Poisson's ratio, G_{xy},G_{yz}, G_{xz} - are shear modules of elasticity in *xy*, *yz*, *xz* planes. If we assume that matrix $\mathbf{E}^{-1}$ is symmetric, then

$$\frac{\nu_{yx}}{E_{yy}}=\frac{\nu_{xy}}{E_{xx}},\ \frac{\nu_{zx}}{E_{yy}}=\frac{\nu_{xz}}{E_{xx}},\ \frac{\nu_{zy}}{E_{zz}}=\frac{\nu_{yz}}{E_{yy}}. \tag{13}$$

For anisotropic case the elasticity matrix $\mathbf{E}$ include 21 independent coefficients. For orthotropic material the elasticity matrix $\mathbf{E}$ include only 9 independent coefficients. The isotropic material is defined by Lame elastic constants

$$\lambda=\frac{\nu E}{(1+\nu)(1-2\nu)}\qquad \mu=\frac{E}{2(1+\nu)}=G\,. \tag{14}$$

The thermal stresses we can compute from (7).

In general we note that calculation of thermal stresses for nonlinear materials is more complicated and use two approaches [7]:

1. Thermo-mechanical analysis.

In this class of problems, the thermal solution can affect the structural solution but the structural solution does not affect the thermal solution. In thermal analysis can be used identical mesh as in structural analysis.

2. Thermo-mechanical coupling.

In this analysis the thermal solution and structural solution affect each other. The thermo-mechanical problems can be included the following effects:

- Internal heat generation due to plastic deformations of the material
- Heat transfer between contacting bodies

3. Finite element model

The commercial FEM code ANSYS was used for numerical analysis. The one-way thermal-mechanical coupling was used, because heat generation due to plastic deformation was neglected against heat generated by weld arc as was stated in [4] or [6]. The welding process was modelled by prescribing temperature and size of molten pool, which was calibrated by experiment. The movement of electrode was modelled by element birth and dead technique.

3.1. Geometrical model

Geometrical model of analysed problem is in fig. 1. Material of pipe and tap was STN 12 022. Inner diameter of pipe was 126 mm, thickness was 8 mm and modelled length of pipe was 300 mm. The tap thickness was 6 mm and length was 150 mm. Width of tap was equal to quarter of pipe circumference. In this model the 1 mm gap between the pipe and tap was considered. The size of fillet weld was 5 mm.

3.2. FEM mesh

For thermal analysis were used SOLID70 and SOLID90 elements. Gradated mapped mesh with linear elements (SOLID70) was used in regions far from thermal gradients and finer free mesh of quadratic elements (SOLID90) was used in region with high thermal gradients (fig. 3). SURF152 elements were used to model radiation and convection boundary conditions.

Same topology of mesh was used for structural analysis, but thermal SOLID70 elements were replaced by structural SOLID45 and thermal SOLID90 by structural SOLID95.

3.3. Boundary conditions

In the thermal analysis convection and radiation boundary conditions are employed. Natural convection between the pipe, tap and surrounding environment was modelled by the film coefficient $h = 6$ Wm^{-2} and convection between inner surface of pipe and flowing compressed gas was modelled by the film coefficient $h = 102.3$ Wm^{-2}. The emissivity of radiating surfaces was $\varepsilon = 0.66$, ambient temperature $T_0 = 20\ ^0$C. Welding speed is $v = 2$ ms^{-1}.

In the structural analysis rigid body modes were removed to obtain residual stresses.

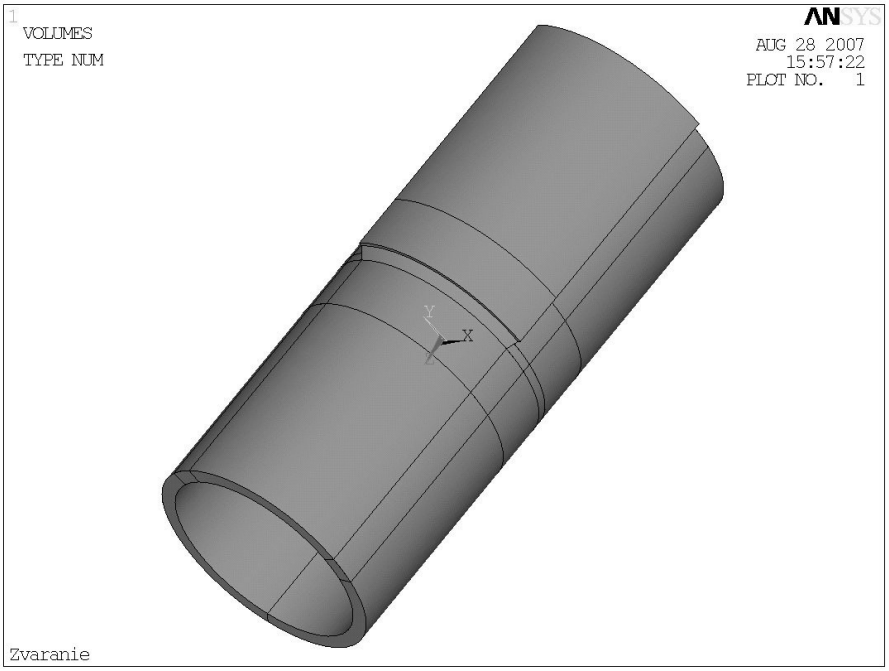

Fig. 2. Geometrical model.

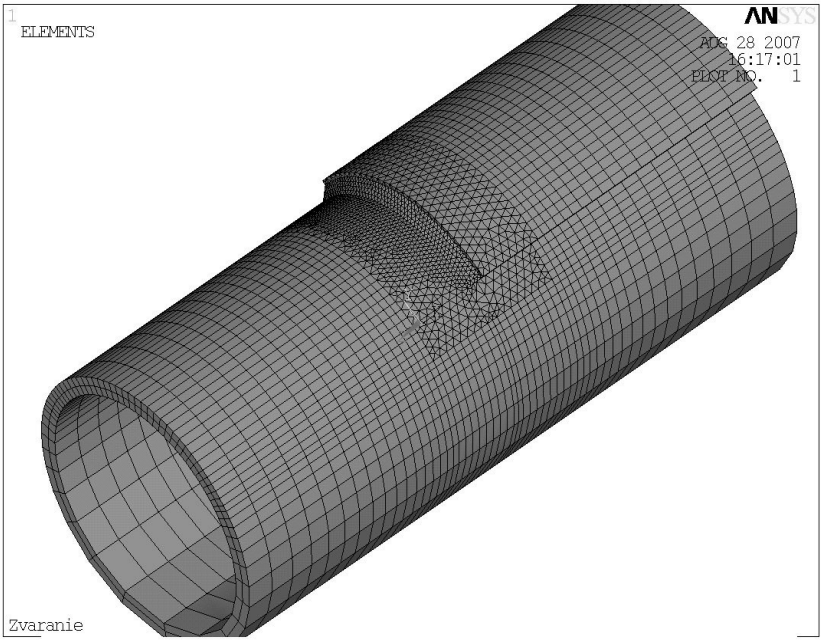

Fig. 3. FE mesh.

3.4. The solution strategy

The one-way coupling strategy based on two separate databases was used. The thermal history was computed first and then structural analysis was conducted using temperatures from thermal analysis as body loads. This strategy speeds up solution.

The modelled length of pipe was chosen such that temperature on both cuts was equal to ambient temperature during welding. When welding was done cooling to ambient temperature was performed.

4. Results

Fig. 5 shows the temperature distribution of the welded parts at middle of welding time, t = 26.311 s and fig. 6 at end of welding time, t = 52.622 s. As can be seen from the figures, the temperature around the weld reaches 1650 ^{0}C suggesting melted material in the fusion zone (FZ). High temperatures are present at immediate vicinities of the FZ, which defines the heat affect zone.

In fig. 7 are graphs of thermal history in points B1, B2, B3. They lying in symmetry plane (in meridian cut through the middle of tap) and their locations are shown in fig. 4. As can be seen in fig. 7, that the calculated temperatures of points B1, B2, B3 are increased almost immediately after the weld arc passes their position. The maximum temperature of point B3 is higher than that of B2 as excepted because B3 is located closer to the weld-pool boundary than B2. Since the change of temperature with time from 800 to 500 ^{0}C is fairly similar for points in the vicinity of the heat source, the cooling time $t_{8/5}$ for B3 is approximately 10 s.

In fig. 8 are graphs of thermal history in points T1 to T5 where the temperatures was measured. They are on the external surface of pipe in a distance of 20 mm from front face of tap and points T4 and T5 lies in a distance of 25 mm from front face of tap. The distance of nodes T1 and T2 is measured along the pipe circumference is 10 mm (the distance between the points T4 and T5 is the same). The welding input data are calibrated according to temperature measurements [4].

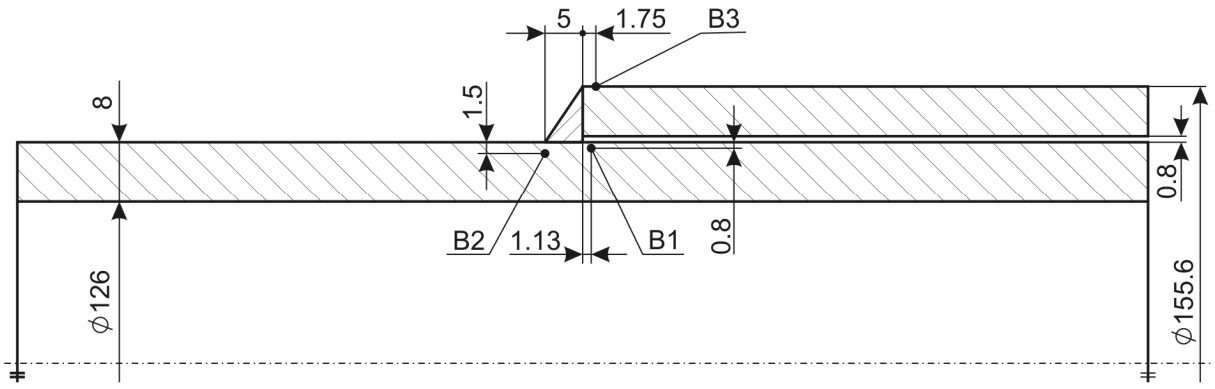

Fig. 4. Placements of points B1, B2 and B3.

In figs. 9 - 12 are described results from thermo-mechanical analysis. In figs. 9 and 10 are values of hoop residual stresses and in figs. 11 and 12 are values Mises stresses on external and inner surface of pipe from thermo-mechanical analysis. The maximum value of hoop stress is 346.342 MPa and maximum Misses stress is 309.831 MPa. These values exceed yield stress of material, which is σ_Y = 295 MPa for steel 12023. Look forward to that these stress values will be lower for thermo-mechanical coupling. Unfortunately, the software ANSYS not enable to perform full thermo-mechanical coupling analysis with internal heat generation due to plastic deformations of the materials.

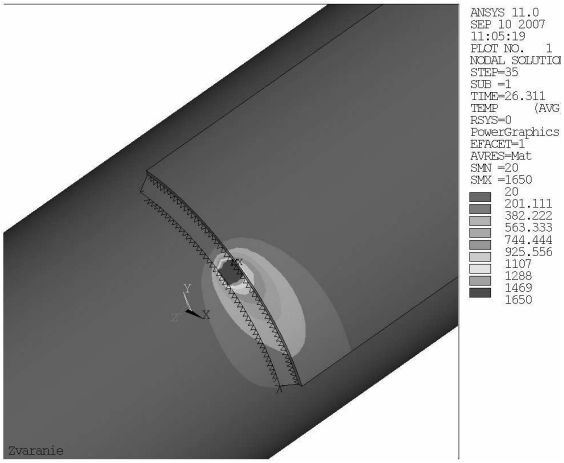

Fig. 5. Temperature field at middle of welding (time 26.311s).

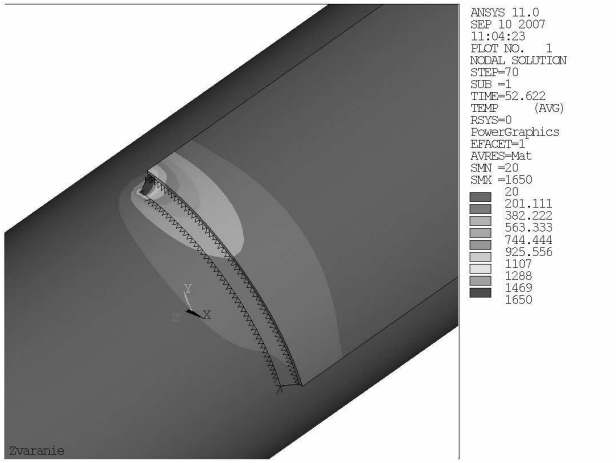

Fig. 6. Temperature field at end of welding (time 52.622 s).

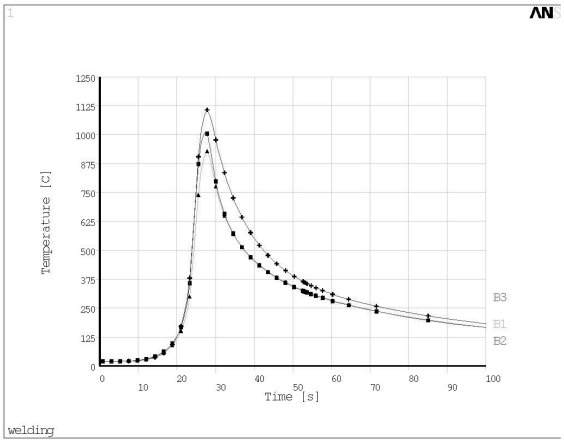

Fig. 7. Thermal history – points B1, B2, B3.

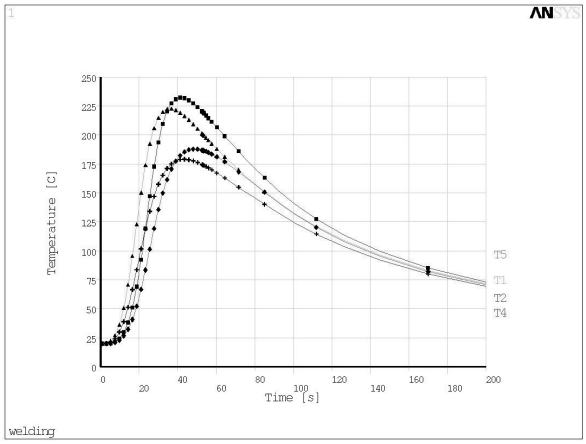

Fig. 8. Thermal history – points T1, T2, T4, T5.

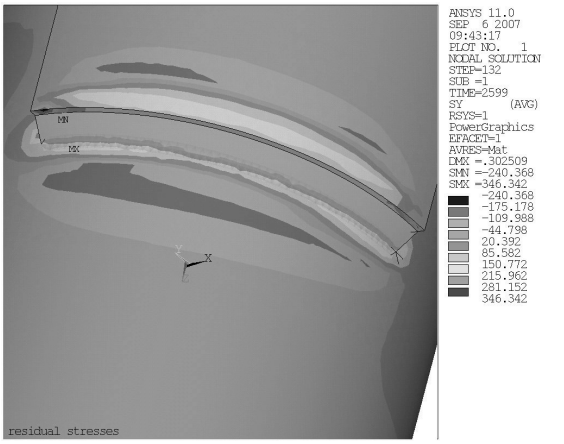

Fig. 9. Hoop stresses – external surface.

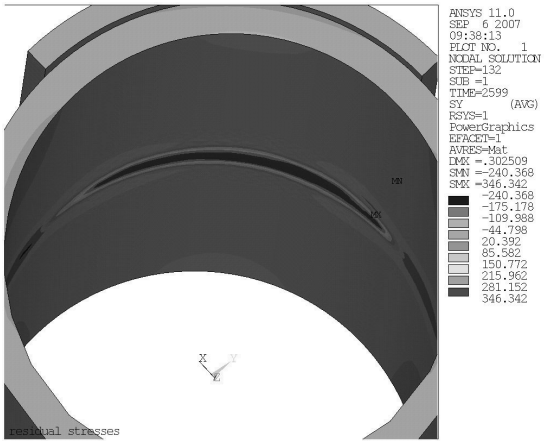

Fig. 10. Hoop stresses – front view.

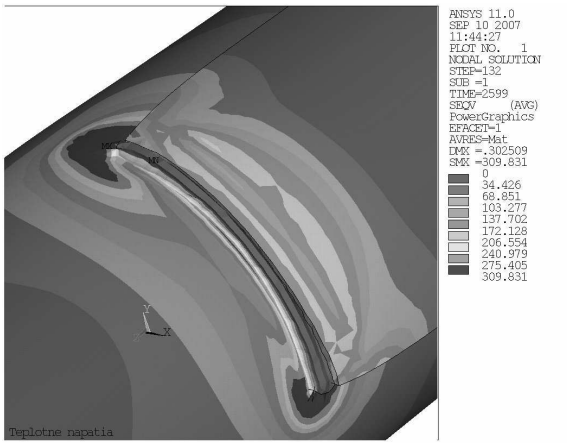

Fig. 11. Mises stresses – external surface.

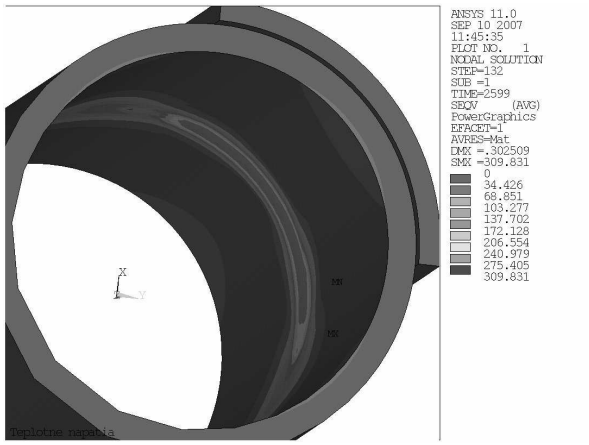

Fig. 12. Mises stresses – front view.

5. Conclusion

The paper has shown that it is possible to simulate the residual stress of in service welding using commercial software ANSYS. Three-dimensional FE models of circumferential welds have been developed. These models have been used to predict weld zone geometries and $t_{8/5}$ weld cooling times. The final microstructure structure tends to presence of phases: Ferrite, Pearlite and Bainite with a hardness cca 190 HV. The predicted values $t_{8/5}$ have shown that it is possible calculate the thermal fields and weld cooling times to a useful accuracy. Welding velocity and cooling by agitated gas have significant influence on temperature field and on temperature $t_{8/5}$ but radiation and surrounding air have only negligible influence.

Acknowledgements

This work has been supported by grant project VEGA-1/2097/05 and APVT-20-00310.

References

[1] L. W. Bang, Y. P. Son, K. H. Oh, Y. P. Kim, W. S. Kim, Numerical simulation of sleeve repair welding of in-service gas pipelines, Welding Journal (2002) 273-282.
[2] P. Elesztös, V. Voštinár, Ľ. Mráz, Numerical and experimental analysis of the deformational and stress state of welded joints, Acta Mechanica Slovaca 1/2006 (2006) 101-108.
[3] M. D. Chapetti, J. L. Otegui, C. Manfredi, C. F. Martins, Full-scale experimental analysis of stress states in sleeve repairs of gas pipelines, Materials Processing Technology 78 (2001) 379-387.
[4] J. Meško, Problematic of discontinuity of circumferential welding joints using T.D. Williamson tapping fittings on high-pressure vessels, Research report, University of Žilina, 2007.
[5] N. T. Nguyen, Thermal analysis of Welds, Wit Press, 2004.
[6] A. S. Oddy, J. A. Goldak, J. M. J. McDill, Transformation plasticity and residual stresses in single-pass repair welds, ASME PVP - Weld residual stresses and plastic deformation 173 (1989) 13-18.
[7] Theory reference for ANSYS and ANSYS workbench, ANSYS release 11, ANSYS Inc., 2007.
[8] A. H. Yaghi, T. H. Hyde, A. A. Becker, J. A. Williams, W. Sun, Residual stress simulation in welded sections of P91 pipes, Materials Processing Technology 167 (2005) 480-487.
[9] M. Žmindák, R. Melicher, P. Novák, Numerical simulation of thermal process in welding, Proceedings of 6th International Scientific Conference Engineering for Rural Developmen, Jelgava, Latvia republic, 2007, pp. 221-225.